2024 IEEE/RSJ International Conference on Intelligent Robots and Systems (IROS)
October 14-18, 2024. Abu Dhabi, UAE

Indoor Position Estimation Using NLoS Reflected Path with Wireless Distance Sensors

Tomoya Itsuka[1] and Ryo Kurazume[2]

***Abstract*— Indoor robot localization is important for the realization of autonomous service robots. Various studies have been conducted on "indoor GPS" measurements using wireless distance sensors such as ultrasonic beacons. However, when these beacons encounter non-line-of-sight (NLoS) conditions due to obstacles, accurate distance measurements become challenging because of multipath and other effects. In this study, we propose a method for simultaneously estimating a robot's position and distance to reflective surfaces in an environment using wireless distance sensors. The proposed method can estimate not only the robot's position but also the reflection of the beacon signal. First, the wheel odometry of the robot is assumed to be the initial value, and the measured distance from the beacon to the robot is used as a factor to construct the factor graph. Second, the distance to the reflective surface of the beacon signal, which is parallel to the robot's movement plane, was estimated from the robot position sequence using the GMM and used as a noise model in the factor graph. Finally, the method is evaluated by acquiring data in a real environment with obstacles. Compared with a method that does not consider reflection paths, this method demonstrated improved accuracy and effectiveness.**

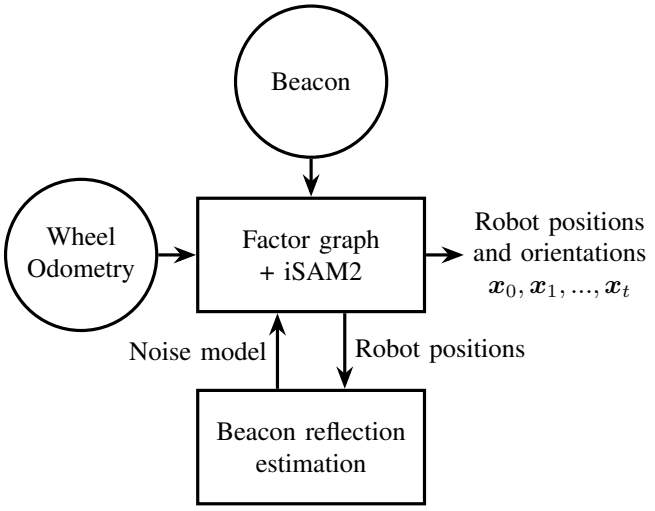

Fig. 1. System Architecture. The proposed method estimates the robot's position and distance to the reflective surface of the beacon signal alternately.

I. INTRODUCTION

Robot position estimation is important for achieving autonomous mobility. Position estimation technology has been widely applied to sensor fusion, in which errors accumulated by internal sensors such as IMU and wheel odometry are compensated for by external sensors such as GPS. In outdoor environments, 3D-LiDAR and GPS-based position estimation have been actively studied for the development of autonomous vehicles. In contrast, indoor environments require precise position estimation due to close proximity to walls and frequent movement of people and obstacles. However, there is a major drawback: GPS is not available and an absolute position cannot be obtained.

Due to the unavailability of GPS for position estimation and SLAM in indoor environments, high-performance correction has been achieved using loop-closing techniques that extract and match features from point clouds using LiDAR and cameras. However, because these methods depend on the surrounding geometry, they are difficult to use in environments with few features (e.g., corridors) or numerous dynamic obstacles in the surroundings. In recent years, with the development of ultra-wideband (UWB) ranging beacons, various studies have been conducted to perform "indoor GPS." SLAM methods that combine LiDAR and beacons have been reported to provide accurate SLAM outcomes even in feature-poor environments such as corridors and tunnels. However, if beacons have non-line-of-sight (NLoS) conditions, in which obstacles exist between beacons, an accurate distance cannot be obtained owing to multipath and other effects. In general, there are two ways to address such NLoS errors: one involves detecting and ignoring the NLoS signal, while the other involves mitigating the NLoS error by including the noise caused by the NLoS in the observation model. Most recently, the non-Gaussian nature of noise in distance sensors has been the focus of particular attention in factor graph-based methods, which have been extremely successful in SLAM, and methods that attempt to reproduce the error function have frequently been used.

Sound source localization (SSL) is a method for estimating sound source locations. Numerous studies have considered sound reflections in the environment. Ultrasonic sound has a strong reflection component owing to its high frequency. Therefore, localization methods that utilize ultrasonic beacons with such reflection paths can be used in complex environments where line of sight (LoS) is not feasible by taking advantage of multiple paths. Although there is a method for robot position estimation that leverages such reflections, setting it up in advance can be challenging. This is due to the requirement of providing an environmentally reflective surface beforehand.

[1]Tomoya Itsuka is with Graduate School of Information Science and Electrical Engineering, Kyushu University, Japan. itsuka@irvs.ait.kyushu-u.ac.jp

[2]Ryo Kurazume is with Faculty of Information Science and Electrical Engineering, Kyushu University, Japan. kurazume@ait.kyushu-u.ac.jp

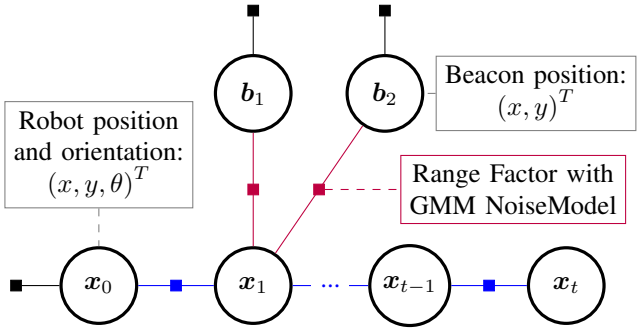

Fig. 2. Overall factor graph. The blue squares are odometry factors, and the black squares are prior factors.

Algorithm 1 Overall method

```
Initialize F with Prior Factors
while true do
    if odometry data is updated then
        Update F with Odometry Factor
    end if
    if beacon data is updated then
        Update F with Range Factor
        Estimate the variables Θ using isam2 solver
            ▷ linearize each range factor (Algorithm 3)
        θ_s^GMM ← esitimate_s(F)            ▷ Algorithm 2
    end if
end while
```

The contributions of this study are as follows:

- We propose a method that can also use multipath signals of ultrasonic beacons in the indoor robot localization task.
- It simultaneously estimates the environmental reflective surfaces necessary to leverage multipath signals. Specifically, it estimates the distribution of distances to reflective surfaces parallel to the 2D plane in which the robot moves using GMM, and the distribution is used to estimate the robot's position.

II. RELATED WORK

Remarkable progress has been achieved in the SLAM of point clouds using 3D-LiDAR and GPS. Among them, LIO-SAM [1] realizes highly accurate SLAM by integrating IMU, GPS, and LiDAR using a factor graph.

In particular, the correction of not only the pose of the robot, but also the intrinsic parameters of the sensors is frequently addressed. For example, in IMU pre-integration [2], the bias term of the IMU is corrected by re-estimating the optimized robot pose sequence, including LiDAR data. In addition, IMU preintegration was used in the LIO-SAM to obtain robust odometry.

Factor graph optimization methods such as the Gauss-Newton method and the Levenberg-Marquadt method have the disadvantage that the estimation time increases exponentially when the number of factors increases sequentially, such as in general slam problems. The ISAM2 solver [3] is sufficiently fast to operate in real-time by determining the parts that should be linearized.

Pfeifer et al. [4] proposed an effective method for addressing NLoS errors when utilizing distance sensors, such as UWB beacons or GPS, as pseudo-range sensors. This method extends the error function in the factor graph to a GMM and simultaneously estimates the attitude of the robot and error distribution of the distance sensor. Importantly, this approach remains effective even when the sensor exhibits an unknown constant bias. Several studies have been conducted to improve iSAM2 and the factors that handle more nonlinear observation noise [5]–[9]. Max-Mixture [8] and Max-sum-mixture [9] are methods that have been extended to allow the GMM to be used in factor-noise models. Max-sum-mixture is also used in the latest UWB beacon-based location estimation method, using the Time Differential of Arrival (TDoA) technique [10].

Incorporating range beacons allows for effective SLAM in environments with limited features, which is difficult when using LiDAR-based SLAM [11], [12]. Previous research has specifically addressed NLoS detection and mitigation to address the NLoS error of range beacons [13]. However, numerous studies on SSL exploit the reflective properties of sound [14]–[16]. In addition, certain studies have actively used multipath signals generated by the NLoS for beacon-based target localization [17], [18]. Kim et al. [17] considered the use of measurements under NLoS conditions and worked on position estimation by considering reflection paths. However, it is necessary to obtain distance measurements from three or more points simultaneously, and the computation time increases with the number of combinations of beacons and environmental walls. Fares et al. [18] proposed localization using a single beacon capable of N reflections by unknown obstacles in the environment. However, this method requires the angle of arrival (AoA) of the target to be known in order to be utilized.

To address this problem, we previously proposed a particle filter-based method in which the beacon observation model is dynamically switched depending on the signal [19]. However, in this method, the ceiling height in the environment should be set in advance and only primary reflections from the ceiling can be used.

III. PROPOSED METHOD

We propose a method that can estimate the robot position and the beacon noise model. The overall architecture of the proposed method is shown in Fig. 1. One ultrasonic beacon is installed on the robot and multiple ultrasonic beacons are installed on the environment side, and the distance between the robot and the environment side beacons is assumed to be measurable from the beacons. Wheel odometry is assumed to be available from the robot.

To integrate the odometry and distance information from the beacon, a factor graph was constructed and pose-graph

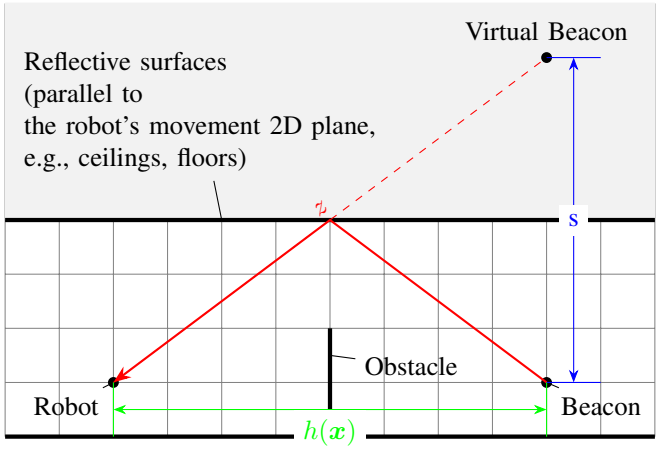

Fig. 3. Environmental reflections, $s^2 = z^2 - h^2(\boldsymbol{x})$

optimization was performed. A factor graph $G = (\mathcal{F}, \Theta, \mathcal{E})$ consists of a variable node $\theta_i \in \Theta$, factor node $f_j \in \mathcal{F}$, and edge e_{ij}. Node f_j is a function of variable θ_i [3].

In this method, the robot pose and beacon position are used as variable nodes. The beacon on the robot side and the beacon on the environment side are placed at the same height, and the robot pose and beacon position are assumed to be on a two-dimensional plane. Three-factor nodes are used: a Prior Factor, which indicates the prior distribution; a Odometry Factor, which indicates the relationship between the robot poses (position and orientation); and a Range Factor, which constrains the distance between the beacon and the robot as measured by the beacon(Fig. 2 and Algorithm 1). Among these, the Prior Factor and Odometry Factor utilize the prior factor and between factor implemented in the gtsam package [20].

The Range Factor was modified to leverage reflection paths caused by environmental surfaces, enabling simultaneous estimation of the reflective surface and robot pose. This method was strongly influenced by the Nested-EM approach [4], which worked on the EM algorithm and the optimization of the factor graph simultaneously.

A. Estimation of environmental reflection surfaces for NLoS multipath

NLoS errors in the beacon measurement distance are primarily caused by measuring the reflection path lengths. These reflective surfaces are difficult to predict accurately because of the large number of flat surfaces in environmental geometry. However, given that the indoor environment in which we live often contains surfaces (ceilings, floors, walls) that can be viewed as static and broad reflective planes, it is possible to estimate the reflection path from the observed data.

The measured distance z from the beacon to the robot is modeled as follows:

$$z = \sqrt{\|\boldsymbol{x} - \boldsymbol{b}\|^2 + s^2} + \eta \tag{1}$$

Algorithm 2 Estimation distances-distribution s of environmental reflection surfaces

1: **function** ESTIMATE_S
2: $\mathcal{S} \leftarrow \emptyset$
3: **for all** Range factor f_i in $\mathcal{F}$ **do**
4: **if** $z_i > h(\boldsymbol{x}_i)$ **then**
5: $s_i \leftarrow \sqrt{z_i^2 - h^2(\boldsymbol{x}_i)}$ ▷ (2)
6: **if** $(s_i > s_{th})$ **then**
7: $\mathcal{S} \leftarrow \mathcal{S} \cup \{s_i\}$
8: **end if**
9: **end if**
10: **end for**
11: **if** size of $\mathcal{S}$ > size threshold **then**
12: Initialize $\boldsymbol{\theta}_s^{GMM} \leftarrow \boldsymbol{\theta}_{s,init}^{GMM}$
13: $\mathcal{S}_w \leftarrow \{s_i \in \mathcal{S} | I - n_w \leq i \leq I\}$ ▷ I is the latest index, n_w is the window size
14: $\boldsymbol{\theta}_s^{GMM} \leftarrow$ EM-method$(\boldsymbol{\theta}_s^{GMM}, \mathcal{S}_w)$
15: **return** $\boldsymbol{\theta}_s^{GMM}$
16: **else**
17: **return** $\emptyset$
18: **end if**
19: **end function**

where $\boldsymbol{x}$ is the true position of the robot, $\boldsymbol{b}$ is the true position of the beacon, and s is the distance between the actual beacon and the mirror reflection image. $\eta \sim \mathcal{N}(0; \sigma_{\epsilon,los}^2)$ is the measurement error. Note that $s = 0$ when there are no obstacles between the robot and beacon.

Assume that the value of the variable node $\boldsymbol{x}_i, \boldsymbol{b}_i$ is a good estimate of the true robot position $\boldsymbol{x}_i$ and beacon position $\boldsymbol{b}_i$, and attempt to estimate s distribution by calculating s using the following equation:

$$s = \sqrt{z^2 - h^2(\boldsymbol{x})} \tag{2}$$

where $h(\boldsymbol{x}) = \|\boldsymbol{x} - \boldsymbol{b}\|^2$ is the distance measurement function. $\boldsymbol{x}$ and $\boldsymbol{b}$ are the positions of the robot and beacon corresponding to the measurement z respectively. Here, s varies depending on the walls and obstacles in the environment, and the positions of the robot and beacon. However, because only a few walls exist in the environment, we assume that the estimated distribution of s can be represented using a GMM. We assume the wall surface in the environment where reflection occurs is a plane parallel to the robot's movement plane (Fig.3). This assumption is valid for ceiling or floor reflection, but may not be valid for walls. Therefore, it may be effective in the center of a room, but not in an environment with close walls, such as a corridor.

To estimate the distribution of s, we compute s from the current estimated $h(\boldsymbol{x})$ for the Range Factor in the Factor graph and store it in $\mathcal{S}$ (Algorithm. 2, line 3-10).

Here, for the observed value z_i, we do not store in $\mathcal{S}$ the observed values that are considered to have been obtained at a direct distance or those that are not considered to be reflection paths. Therefore, a threshold value S_{th} is

Algorithm 3 Linearize a range factor

1: **function** LINEARIZE
2: $\boldsymbol{\theta}_{\epsilon}^{GMM} \leftarrow \{\boldsymbol{\theta}_{\epsilon,0}\}$
3: **for all** $\boldsymbol{\theta}_{s,j} \in \boldsymbol{\theta}_{s}^{GMM}$ **do**
4: $\boldsymbol{\theta}_{\epsilon,j} := (w_{\epsilon,j}, \mu_{\epsilon,j}, \sigma_{\epsilon,j})$ using (8)-(10)
5: $\boldsymbol{\theta}_{\epsilon}^{GMM} \leftarrow \boldsymbol{\theta}_{\epsilon}^{GMM} \cup \{\boldsymbol{\theta}_{\epsilon,j}\}$
6: **end for**
7: Linearize by Max-Mixture with $\boldsymbol{\theta}_{\epsilon}^{GMM}$
8: Weighten by Tukey-Loss
9: **end function**

established and $z_i > h(\boldsymbol{x}_i)$ is required(Algorithm. 2, line 4-6). In addition, a sliding window is used for $\mathcal{S}$ to reduce estimation time. If the size of $\mathcal{S}$ exceeds a certain size, the elements are deleted from the oldest values and the size of $\mathcal{S}$ is kept constant.

We apply the EM algorithm to $\mathcal{S}$ to estimate the GMM parameters $\boldsymbol{\theta}_{s}^{GMM} = \{w_{s,j}, \mu_{s,j}, \sigma_{\epsilon,j}\}$. Beacon measurements within the sliding window and the estimated position of the robot were used as inputs for the EM algorithm. In the experiment, EM estimation was started some time after the start time, and the wheel odometry values were used as is until then.

B. Linearize method

In this section, we convert the calculated GMM reflective distance model, $\boldsymbol{\theta}_{s}^{GMM}$, to a GMM error model for the current estimate, $\boldsymbol{\theta}_{\epsilon}^{GMM}$. Transform GMM $\boldsymbol{\theta}_{s}^{GMM}$ in the direction from the beacon to the robot $\boldsymbol{\theta}_{\epsilon}^{GMM} = \{w_{\epsilon,j}, \mu_{\epsilon,j}, \sigma_{\epsilon,j}\}$

From (2), the error ϵ is given by

$$z = h(\boldsymbol{x}) + \epsilon = \sqrt{s^2 + h^2(\boldsymbol{x})} \tag{3}$$

$$\epsilon(s) = \sqrt{s^2 + h^2(\boldsymbol{x})} - h(\boldsymbol{x}) \tag{4}$$

The first-order approximation using the Taylor expansion of (4) around $s = \mu_s$ is as follows:

$$\frac{\partial \epsilon}{\partial s} = \frac{s}{\sqrt{s^2 + h^2(\boldsymbol{x})}} \tag{5}$$

$$\epsilon(\mu_s + \Delta s) \simeq \left(\sqrt{\mu_s^2 + h^2(\boldsymbol{x})} - h(\boldsymbol{x})\right) \tag{6}$$

$$+\Delta s \frac{\mu_s}{\sqrt{\mu_s^2 + h^2(\boldsymbol{x})}} \tag{7}$$

From (7), the following transformations are performed for each jth component $\boldsymbol{\theta}_{\epsilon,j}$ of the GMM: We assume that the first component $\boldsymbol{\theta}_{\epsilon,0} = \{w_{\epsilon,0}, \mu_\epsilon = 0, \sigma_{\epsilon,los}\}$ contains the measurement error $\sigma_{\epsilon,los}$ of the beacon measurements.

$$w_{\epsilon,j} \leftarrow w_s \cdot (1 - w_{\epsilon,0}) \tag{8}$$

$$\mu_{\epsilon,j} \leftarrow \sqrt{\mu_s^2 + h^2(\boldsymbol{x})} - h(\boldsymbol{x}) \tag{9}$$

$$\sigma_{\epsilon,j} \leftarrow \max\left(\sigma_{\epsilon,los}, \frac{\mu_s}{\sqrt{\mu_s^2 + h^2(\boldsymbol{x})}}\sigma_s\right) \tag{10}$$

(a) Robot (b) Beacon (c) 3D-LiDAR

Fig. 4. The hardware used in the experiment. (a) and (b) were used as input for the proposed method, and (c) was used for groundtruth robot position.

TABLE I
HARDWARE SPECS

Item	Model
Base robot	SEGWAY Loomo
Ultrasonic beacon	Marvelmind Super-Beacon
3D-LiDAR (groundtruth)	Quanergy M8 LiDAR Sensor
PC	Intel Core i9-14900KF (24 core)

The robot, beacon, and 3D-LiDAR were used to acquire the dataset. The PC was used to evaluate the proposed method.

Here, the standard deviation of the error distribution $\sigma_{\epsilon,j}$ is (10) because it is not reduced below the measurement error $\sigma_{\epsilon,los}$ of the beacon during line of sight.

Following the transformation, the Max-Mixture [8] is used to whiten the GMM noise model $\boldsymbol{\theta}_{\epsilon}^{GMM}$, implemented in [4] eq.(9). Tukey loss weighting was also employed to reduce the impact of errors resulting from reflections off new surfaces and unknown measurement errors. This function was also used for the initial estimation where the GMM could not estimate NLoS reflections because of a lack of beacon measurements.

The linearization step is presented in Algorithm 3. This linearization step was re-performed using fluid relinearization, which is a feature of the iSAM2 solver [3]. This linearization allows the currently estimated GMM model to be retroactively reapplied to past Range Factors.

IV. EXPERIMENT

The hardware used in the experiment (Fig. 4 and Tab. I). The robot was equipped with a beacon(Fig. 4a). Wheel odometry was performed using Loomo API. The beacon setup uses the Inverse Architecture setup (IA), where the beacon on the environment side emits a specific frequency, and the beacon on the robot side receives it. Two 3D LiDARs were deployed in the newly acquired dataset to obtain the ground truth of the robot position in the environment.

The experimental setup is depicted in Fig. 5. Fig. 6a illustrates an environment without obstacles and Fig. 6b presents the environment with obstacles. Four ultrasonic beacons were installed, and their distances from the beacons were obtained. Wheel odometry values were obtained from the robot.

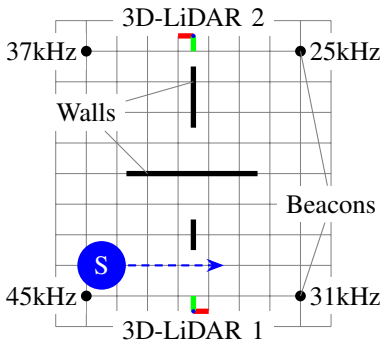

Fig. 5. Environmental map. The S is the robot's start point. The cell size is 1m x 1m. Four beacons are placed at the corners of a 7m x 8m square.

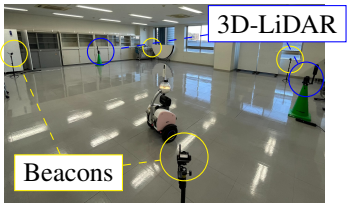

(a) Environment without obstacles

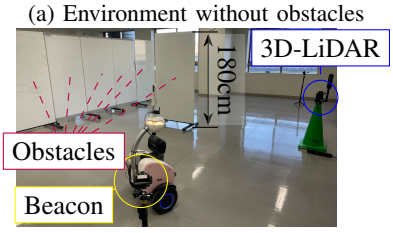

(b) Environment

Fig. 6. Experimental environment. The ceiling height is $259cm$.

Two 3D-LiDARs were also installed in this environment to obtain the true values of the robot; these 3D-LiDARs performed differential detection by dropping the dimensions of the point cloud onto the xy-plane, and the trajectory of the robot was obtained by clustering using DBSCAN.

The location estimation calculations were verified on a desktop PC equipped with an i9-14900KF (24 cores and 32 threads). Factor graphs and iSAM2 were generated using GTSAM [20], and GMM estimation was performed using MLPACK [21]. In addition, part of the implementation was parallelized using OpenMP. The hyperparameters are listed in Tables III and II. The beacon location variable is constrained. It is given in advance and is not updated in the estimation. K-means was used to initialize the GMM estimation, and the previous estimation results were used for the second and subsequent estimations.

Twenty initial poses of the robot are generated using a normal distribution: $(\sigma_x^2, \sigma_y^2, \sigma_\theta^2) = (0.25\mathrm{m}^2, 0.25\mathrm{m}^2, 0.030\mathrm{rad}^2)$ around the starting position, and estimation was performed for each initial pose. In this experiment, four estimation methods were compared(Table IV). The accuracy of estimating the distribution of the initial poses was evaluated (Table V, Table VI).

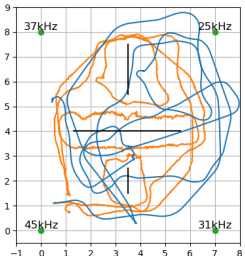

Fig. 7. Wheel odometry and groundtruth. The blue trajectory is the wheel odometry. The orange trajectory is the groundtruth.

TABLE II
HYPER PARAMETERS

Parameter	Value
Range Factor	
$w_{\epsilon,0}$	0.5
$\mu_{\epsilon,0}$	0 m
$\sigma_{\epsilon,0} = \sigma_{\epsilon,los}$	0.1 m
$\mathcal{S}$ size threshold in Alg. 2	30
$\mathcal{S}$ max window size	500
GMM estimation start time	15 sec after start time
Maximum component size of $\boldsymbol{\theta}_s^{GMM}$	3
Initial estimate $\boldsymbol{\theta}_s^{GMM}$	k-means
Maximum component size of $\boldsymbol{\theta}_\epsilon^{GMM}$	4
Tukey-weight	2.0
isam2 relinearize threshold	0.01

TABLE III
FACTOR COVARIANCE

Factor	Covariance Matrix Σ
Odometry Factor (Wheel Odometry)	$\mathrm{diag}(0.0005\,\mathrm{m}^2, 0.0005\mathrm{m}^2, 0.055\mathrm{rad}^2)$
Range Factor	$0.01\mathrm{m}^2$
Beacon Prior Factor	Constrained
Robot Pose Prior Factor	$\mathrm{diag}(0.01\mathrm{m}^2, 0.01\mathrm{m}^2, 0.01\mathrm{rad}^2)$

A. Accuracy

The absolute trajectory error (ATE) is used to evaluate the proposed method.

$$ATE(X, X^*) = \sqrt{\frac{1}{N}\sum_{i=0}^{N-1} \|\boldsymbol{x}_i^* - \boldsymbol{x}_i\|^2} \tag{11}$$

Here, $X^* = \{\boldsymbol{x}_0^*, \boldsymbol{x}_1^*, ..., \boldsymbol{x}_{N-1}^*\}, \boldsymbol{x}_i^* := (x_i^*, y_i^*)$ is the robot position by 3D-LiDAR as ground truth, and $X = \{\boldsymbol{x}_0, \boldsymbol{x}_1, ..., \boldsymbol{x}_{N-1}\}, \boldsymbol{x}_i := (x_i, y_i)$ is estimated robot position. Two types of ATE were computed: one was the current position of the robot estimated at each time point. The second is the robot trajectory estimated at the last time point.

The results of the study are shown in Table V. Overall, the proposed method exhibited the best performance.

One remaining issue is the accurate estimation of the initial position, which may be challenging if the initial position is off, potentially performing worse than odometry depending

TABLE IV
METHOD COMPARISON

Method	Wheel Odometry	Range Factor	Range Factor+GMM	Proposed method
Wheel odometry	✓	✓	✓	✓
Range Factor with Tukey-Loss		✓	✓	✓
Convert to s				✓
GMM noisemodel & Nested-EM method			✓	✓
Add mean 0 GMM component			✓	✓
Transformation from $\boldsymbol{\theta}_s^{GMM}$ to $\boldsymbol{\theta}_\epsilon^{GMM}$				✓

TABLE V
ABSOLUTE TRAJECTORY ERROR (ATE) $[m]$

Method	mean	std	min
Wheel odometry	1.94	0.40	1.45
Range factor (each time)	8.47	4.75	1.18
Range + GMM (each time)	2.63	3.04	0.73
Proposed method (each time)	**1.84**	2.01	**0.39**
Range factor (latest)	8.43	4.75	1.11
Range + GMM (latest)	2.50	3.00	0.68
Proposed method (latest)	**1.73**	2.02	**0.39**

TABLE VI
PROCESSING TIME $[s]$

	Total[a]		Per Iteration[b] (mean)	
Method	mean	std	ISAM2	GMM-EM
Range factor	26.31	19.29	0.0018	–
Range + GMM	156.89	25.15	0.0051	0.10
Proposed method	100.94	15.36	0.0075	0.06

The dataset duration is 415 s. The odometry data size is 2719 (6.6Hz), and the beacon data size is 5537 (13.3Hz, 4.4Hz for each beacon).
[a] Total denotes the duration of the estimation for the entire dataset.
[b] Per Iteration indicates the duration of one ISAM2 update or the time taken for one GMM EM-method.

on the initial pose set. Therefore, the high dependence of position estimation on the initial pose is a future issue.

B. Computation Time

The time required for the estimation was measured. The overall times required are listed in Table VI. The estimation method using the GMM EM-method increased the computation time with a window size of $\mathcal{S}$.

It was observed that the larger the window size, the more past reflections can be considered; however, the trade-off is that the estimation time increases.

C. Discussion

The wheel odometry trajectory is shown in Fig. 7. And the best-estimated trajectories for Odometry, Range Factor+GMM, and Proposed method are shown in Fig. 8. From the image, it can be observed that the proposed method shows a trajectory closest to the true value.

The error distribution of the best estimation of Range Factor+GMM is illustrated in Fig. 9 and that of the proposed method is illustrated in Fig. 10. Once the image was converted to s, the GMM estimation of the error distribution became more convergent. This is thought to improve the estimation accuracy.

Fig. 11 shows the actual beacon distance measurements and the use of NLoS multipath reflections by the noise model of the proposed method. Even though the measured distance jumps due to NLoS, they can be used as reflections by estimating the $\boldsymbol{\theta}_s^{GMM}$.

The number of elements in GMM is currently fixed using the k-means method. In future studies, the number of elements will be dynamically adjusted to select the number of elements according to the situation.

D. Limitation

This method appears to be effective for indoor rooms, such as the one used in the experiment, particularly for environments where ceiling and floor reflections are dominant. However, it is necessary to confirm whether this method is effective for indoor environments such as corridors, which are surrounded by walls and have a limited number of beacons.

Furthermore, the effectiveness of this method in dynamic environments is a topic for future research.

V. CONCLUSIONS

To address the NLoS error of ultrasonic beacons, this study proposes a method for simultaneously estimating a robot's position and distance to reflective surfaces in the environment. By estimating the reflective surface using the GMM, we realized a position estimation method that effectively utilizes the reflective path owing to the multipath. In the future, we plan to accelerate the processing time to enable real-time operations and address the estimation accuracy degradation caused by the initial position.

ACKNOWLEDGMENT

This work was partially supported by JST, the establishment of university fellowships towards the creation of science technology innovation, Grant Number JPMJFS2132, JSPS KAKENHI Grant Numbers JP20H00230, and a collaborative research with KYOCERA Corporation.

REFERENCES

[1] T. Shan *et al.*, "Lio-sam: Tightly-coupled lidar inertial odometry via smoothing and mapping," in *2020 IEEE/RSJ International Conference on Intelligent Robots and Systems (IROS)*, 2020, pp. 5135–5142.

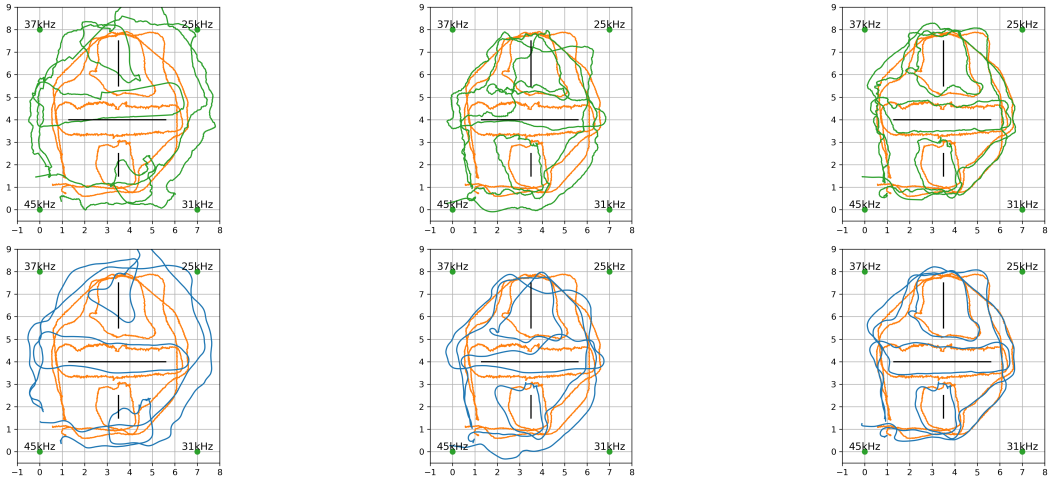

(a) Range factor (ATE:1.11m) (b) Range+GMM (ATE:0.68m) (c) Proposed method (ATE:0.39m)

Fig. 8. Estimated trajectory. The orange trajectory is groundtruth, the green trajectory is the current positions estimated at each time point, and the blue trajectory estimated at the last time point.

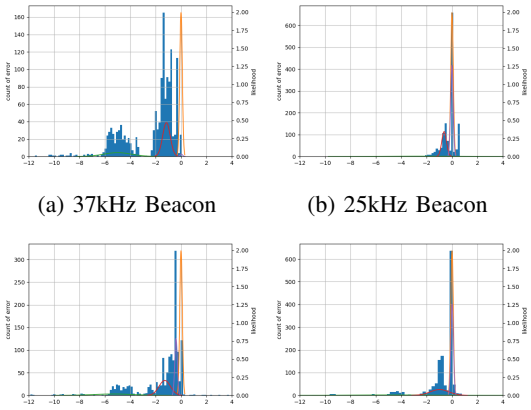

(a) 37kHz Beacon (b) 25kHz Beacon

(c) 45kHz Beacon (d) 31kHz Beacon

Fig. 9. Noise distribution of Range + GMM method. The distribution of $\epsilon = h(\boldsymbol{x}) - z$. The orange Gaussian component is the added mean 0 component.

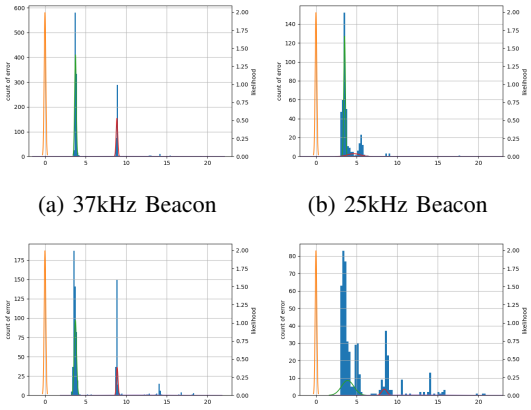

(a) 37kHz Beacon (b) 25kHz Beacon

(c) 45kHz Beacon (d) 31kHz Beacon

Fig. 10. Noise distribution of Proposed method. The distribution of $s = \sqrt{z^2 - h^2(\boldsymbol{x})}$. The orange Gaussian component is the added mean 0 component. This histogram is calculated from beacon measurements $\{z_1, ..., z_T\}$ and latest estimated positions $\{\boldsymbol{x}_1, ..., \boldsymbol{x}_T\}$. (a) and (b) are well converged and show similar distribution shapes.

[2] C. Forster, L. Carlone, F. Dellaert, and D. Scaramuzza, "On-Manifold Preintegration for Real-Time VisualInertial Odometry," *IEEE Transactions on Robotics*, vol. 33, no. 1, pp. 1–21, Feb. 2017, iEEE Transactions on Robotics.

[3] M. Kaess *et al.*, "iSAM2: Incremental smoothing and mapping with fluid relinearization and incremental variable reordering," in *2011 IEEE International Conference on Robotics and Automation*, May 2011, pp. 3281–3288.

[4] T. Pfeifer and P. Protzel, "Expectation-Maximization for Adaptive Mixture Models in Graph Optimization," in *2019 International Conference on Robotics and Automation (ICRA)*. Montreal, QC, Canada: IEEE, May 2019, pp. 3151–3157.

[5] D. Fourie, *Multi-modal and inertial sensor solutions for navigation-type factor graphs*. Woods Hole, MA: Massachusetts Institute of Technology and Woods Hole Oceanographic Institution, 2017.

[6] M. Hsiao and M. Kaess, "MH-iSAM2: Multi-hypothesis iSAM using Bayes Tree and Hypo-tree," in *2019 International Conference on Robotics and Automation (ICRA)*, May 2019, pp. 1274–1280, iSSN: 2577-087X.

[7] Q. Huang, C. Pu, D. Fourie, K. Khosoussi, J. P. How, and J. J. Leonard, "NF-iSAM: Incremental Smoothing and Mapping via Normalizing Flows," in *2021 IEEE International Conference on Robotics and Automation (ICRA)*. Xi'an, China: IEEE, May 2021, pp. 1095–1102.

[8] E. Olson and P. Agarwal, "Inference on networks of mixtures for robust robot mapping," *The International Journal of Robotics Research*, vol. 32, no. 7, pp. 826–840, 2013.

[9] T. Pfeifer, S. Lange, and P. Protzel, "Advancing Mixture Models for Least Squares Optimization," *IEEE Robotics and Automation Letters*, vol. 6, no. 2, pp. 3941–3948, Apr. 2021, conference Name: IEEE Robotics and Automation Letters.

[10] W. Zhao, A. Goudar, M. Tang, X. Qiao, and A. P. Schoellig, "Uncertainty-Aware Gaussian Mixture Model for UWB Time Difference of Arrival Localization in Cluttered Environments," in *2023 IEEE/RSJ International Conference on Intelligent Robots and Systems (IROS)*, Oct. 2023, pp. 5266–5273.

[11] Y. Song *et al.*, "UWB/LiDAR Fusion For Cooperative Range-Only SLAM," in *2019 International Conference on Robotics and Automation (ICRA)*. IEEE, may 2019, pp. 6568–6574.

[12] W. Zhen and S. Scherer, "Estimating the Localizability in Tunnel-like Environments using LiDAR and UWB," in *2019 International Conference on Robotics and Automation (ICRA)*. IEEE, may 2019, pp. 4903–4908.

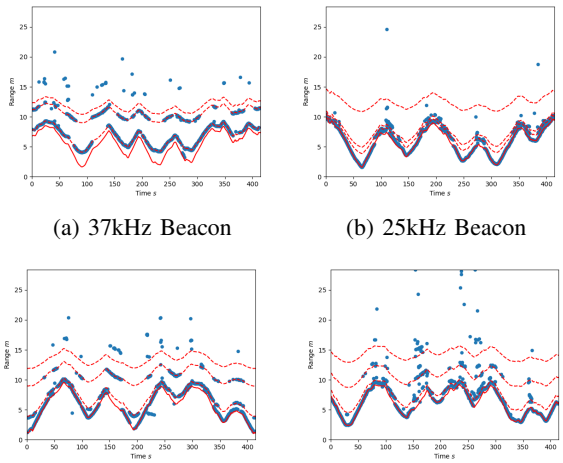

(a) 37kHz Beacon (b) 25kHz Beacon

(c) 45kHz Beacon (d) 31kHz Beacon

Fig. 11. Estimation results of the s distribution via the GMM noise model. The horizontal axis denotes time, and the vertical axis denotes distance. The blue plots are the distances measured from each beacon. The solid red line is the predicted distance from the robot to the beacon calculated from the estimated trajectory. The red dashed line is plotted using the means $\mu_{s,i}$ of the GMM distribution $\boldsymbol{\theta}_s^{GMM}, \sqrt{\mu_{s,i}^2 + h^2(\boldsymbol{x})}$. For instance, measurements with continuous reflection paths were obtained for 150–170 s (c), and these measurements were approximated by the GMM.

[13] J. Khodjaev *et al.*, "Survey of NLOS identification and error mitigation problems in UWB-based positioning algorithms for dense environments," *annals of telecommunications - annales des télécommunications*, vol. 65, no. 5-6, pp. 301–311, jun 2010.

[14] G. Narang *et al.*, "Auditory-aware navigation for mobile robots based on reflection-robust sound source localization and visual SLAM," in *2014 IEEE International Conference on Systems, Man, and Cybernetics (SMC)*, Oct. 2014, pp. 4021–4026, iSSN: 1062-922X.

[15] K. Takami *et al.*, "Non-field-of-view sound source localization using diffraction and reflection signals," in *2016 IEEE/RSJ International Conference on Intelligent Robots and Systems (IROS)*. Daejeon: IEEE, Oct. 2016, pp. 157–162.

[16] I. An, Y. Kwon, and S.-e. Yoon, "Diffraction- and Reflection-Aware Multiple Sound Source Localization," *IEEE Transactions on Robotics*, vol. 38, no. 3, pp. 1925–1944, Jun. 2022, conference Name: IEEE Transactions on Robotics.

[17] K.-W. Kim, J. Kwon, C.-G. Lee, and J. Han, "Accurate Indoor Location Tracking Exploiting Ultrasonic Reflections," *IEEE Sensors Journal*, vol. 16, no. 24, pp. 9075–9088, Feb. 2016, conference Name: IEEE Sensors Journal.

[18] M. H. Fares, H. Moradi, M. Shahabadi, and Y. Mohanna, "Beacon-Based Approach for Target Localization in NLOS Condition for N-Bounce reflections," in *2021 IEEE 4th International Conference on Computing, Power and Communication Technologies (GUCON)*. Kuala Lumpur, Malaysia: IEEE, Sep. 2021, pp. 1–6.

[19] T. Itsuka and R. Kurazume, "Indoor Position Estimation using NLoS Information by Wireless Distance Sensors," in *SII 2023*. Atlanta, GA, USA: IEEE, Jan. 2023, pp. 188–193.

[20] F. Dellaert and GTSAM Contributors, "borglab/gtsam," May 2022. [Online]. Available: https://github.com/borglab/gtsam

[21] R. R. Curtin *et al.*, "mlpack 4: a fast, header-only c++ machine learning library," *Journal of Open Source Software*, vol. 8, no. 82, p. 5026, 2023.